

---

# JOURNAL OF THE AMERICAN CHEMICAL SOCIETY

---

## Discrimination between $^{16}\text{O}$ and $^{18}\text{O}$ in Oxygen Binding to the Reversible Oxygen Carriers Hemoglobin, Myoglobin, Hemerythrin, and Hemocyanin: A New Probe for Oxygen Binding and Reductive Activation by Proteins

Gaochao Tian<sup>†</sup> and Judith P. Klinman\*

Contribution from the Department of Chemistry, University of California, Berkeley, California 94720

Received February 9, 1993<sup>⊙</sup>

**Abstract:** A method for the measurement of discrimination between  $^{16}\text{O}$  and  $^{18}\text{O}$  in the reversible interaction of dioxygen with proteins is described. According to this method, total dioxygen ( $\pm$  protein) in reaction vessels is converted to carbon dioxide and analyzed by isotope ratio mass spectrometry. We see a trend in equilibrium isotope effects in proceeding from ancestral oxygen carriers, hemocyanin and hemerythrin,  $^{18}(K)_{\text{obs}} = 1.0184$  and  $1.0113$ , respectively, to myoglobin and hemoglobin,  $^{18}(K)_{\text{obs}} = 1.0054$  and  $1.0039$ , respectively. Oxygen isotope effects have also been calculated by using available frequencies and force constants for dioxygen and various forms of superoxide and peroxide. These computations indicate a discrimination between  $^{16}\text{O}$  and  $^{18}\text{O}$  of ca. 3% for each 0.5 reduction in the bond order of the dioxygen bond. Protonation and concomitant reduction of dioxygen to form superoxide ( $\text{HO}_2^{\cdot}$ ) and peroxide ( $\text{H}_2\text{O}_2$ ) lead to small normal isotope effects of ca. 1%. Comparison of computed and measured isotope effects to known structures for bound dioxygen in hemocyanin, hemerythrin, hemoglobin, and myoglobin provides a frame of reference for further investigations of  $^{18}\text{O}$  isotope effects in oxygen-dependent reactions.

### Introduction

A very large number of proteins either bind dioxygen reversibly or activate dioxygen through reductive processes to yield intermediates capable of the functionalization of organic substrates. The structures and mechanisms of these processes can be studied, in selected situations, via a variety of spectroscopic probes. More often, however, dioxygen derived intermediates are short-lived, precluding their direct detection and characterization.

Isotope effects have played a very prominent role in the study of reaction mechanism, both in solution and in enzyme-catalyzed processes. Hydrogen isotope effects have featured prominently in these studies, due to their ease of measurement and large size.

We have now initiated a program aimed at quantitating both equilibrium and kinetic isotope effects in dioxygen dependent processes through the discrimination between  $^{16}\text{O}$  and  $^{18}\text{O}$ . Although these isotope effects are expected to be quite small, less than 6–7% maximally,<sup>1</sup> they can be accurately and reproducibly measured by conversion of dioxygen to carbon dioxide and determination of  $^{16}\text{O}$  and  $^{18}\text{O}$  ratios by mass ratio spectrometry.<sup>2</sup>

A large number of enzymes catalyzing oxygen insertion into organic substrates [e.g. monooxygenases and dioxygenases<sup>3</sup>] utilize metal ions as the center for oxygen activation. Prior to mechanistic investigations of kinetic isotope effects in these processes, it is necessary to have a frame of reference for the

(1) Klinman, J. P. *Adv. Enzymol.* **1978**, *46*, 415–494.

(2) Guy, R. D.; Berry, J. A.; Fogel, M. L.; Hoering, T. C. *Planta* **1990**, *77*, 483–491.

(3) Hayashi, O., Ed. *Molecular Mechanisms of Oxygen Activation*; Academic Press: New York, 1980.

\* Author to whom correspondence should be addressed.

<sup>†</sup> Present Address: Glaxo Inc., Building 3, # 3095, 3 Moore Drive, Research Triangle Park, NC 27709.

<sup>⊙</sup> Abstract published in *Advance ACS Abstracts*, August 15, 1993.

magnitude of equilibrium isotope effects in the reversible formation of a variety of metal complexes. Among reversible dioxygen carriers found in nature, considerable data exist documenting the nature of the copper (hemocyanin) and iron (hemerythrin, hemoglobin, and myoglobin) dioxygen complexes. In the present study we have measured equilibrium oxygen-18 isotope effects in each of these systems, observing a wide range of values. In order to provide a theoretical context for the interpretation of the experimental data, equilibrium isotope effects have also been computed with use of literature values of frequencies and force constants for dioxygen, superoxide, and peroxide. As shown herein, proposed structures for the dioxygen complexes of hemocyanin, hemerythrin, hemoglobin, and myoglobin can be directly related to our measured and computed equilibrium oxygen-18 isotope effects.

### Experimental Section

**Materials.** All reagents were of the highest purity possible. Horse heart hemoglobin and sperm whale myoglobin were purchased from Sigma. Their purity was checked by sodium dodecylsulfate (SDS) polyacrylamide gel electrophoresis and the proteins were used without further purification. Horseshoe crabs (*Limulus polyphemus* L.), used in the preparation of hemocyanin, and worms (*Phascolopsis gouldii*), used for the preparation of hemerythrin, were from Woods Hole Marine Biological Laboratory. The standard iron solution for atomic absorption was from Fischer.

(a) **Preparation of the Ferrous Forms of Myoglobin and Hemoglobin for Isotope Effect Measurements.** Proteins purchased from Sigma were in the ferric form as indicated by the absence of  $\alpha$  and  $\beta$  bands in the UV-visible spectra.<sup>4</sup> A concentrated protein stock solution (ca. 2 mM) was first dialyzed overnight in 0.010 M Tris-HCl buffer, pH 7.8. Catalase (ca. 2  $\mu$ g/mL) and a slightly less than stoichiometric amount of sodium dithionite were added and the mixture immediately passed through a desalting column equilibrated with the Tris-HCl buffer. Protein was collected and stored on ice prior to use.

(b) **Preparation of Hemocyanin.** A procedure similar to that of Brenowitz et al.<sup>5</sup> was used to isolate oxyhemocyanin from horseshoe crabs. Twelve medium size crabs were bled by cardiac puncture. About 100 mL of blood was collected from each crab. The blood was first centrifuged at 12 000 rpm in a Du Pont Sorvall RC-5B centrifuge with a SS-34 rotor. The supernatant was then centrifuged at 40 000 rpm overnight in a Du Pont Sorvall ultracentrifuge with a rotor T-865 to precipitate hemocyanin. Hemocyanin pellets were dissolved in 0.01 M Tris-HCl buffer, pH 7.8, and dialyzed against the same buffer. After dialysis, hemocyanin was stored on ice until use. The purity, as ascertained by SDS gel electrophoresis, was at least 98%.

(c) **Preparation of Hemerythrin.** A modification of the method from Garbett et al.<sup>6</sup> was used to isolate hemerythrin from *Phascolopsis gouldii*. The worms were obtained live from the Woods Hole Marine Biological Laboratory by next day mail and inspected for gross damage upon arrival. The specimens were maintained at 4 °C in a cold room prior to the start of the procedure. An incision was made in the lower third of each worm and the blood was drained through cheesecloth into iced Erlenmeyer flasks. The pooled raw blood was allowed to sit at 4 °C for ca 1 h and then filtered through glass wool. The filtered blood was centrifuged at 14 000 rpm in a Du Pont Sorvall RC-5B centrifuge with a SS-34 rotor for 15 min. The supernatant and the top white layer were removed and the cells were re-suspended in a 2.5% by weight aqueous NaCl solution. Centrifugal removal of the supernatant and top layer and re-suspension were repeated until no white layer was evident. The cells were then re-suspended with a minimal amount of the 2.5% NaCl solution and were lysed by addition of an equal volume of distilled water followed by stirring at 4 °C overnight. The oxyhemerythrin was separated from cell debris in a Du Pont ultracentrifuge with a Sorvall T-865 rotor at 33 000 rpm for 90 min. Following the ultracentrifugation, protein was crystallized by dialysis at 4 °C against a 15% ethanol in 0.01 M Tris-SO<sub>4</sub><sup>2-</sup> buffer, pH 7.7. The crystals were collected by centrifugation, washed with the crystallization buffer, and finally dissolved and dialyzed in Tris-HCl, pH 7.8.

(4) Antonini, E.; Brunori, M. *Hemoglobin and Myoglobin and their Reactions with Ligands*; North Holland Publishing Co.: Amsterdam, 1971.

(5) Brenowitz, M.; Bonaventura, C.; Bonaventura, J.; Gianazza, Z. *Arch. Biochem. Biophys.* **1981**, *210*, 748-761.

(6) Garbett, K.; Darnall, D. W.; Klotz, I. M.; Williams, R. J. P. *Arch. Biochem. Biophys.* **1969**, *135*, 419-434.

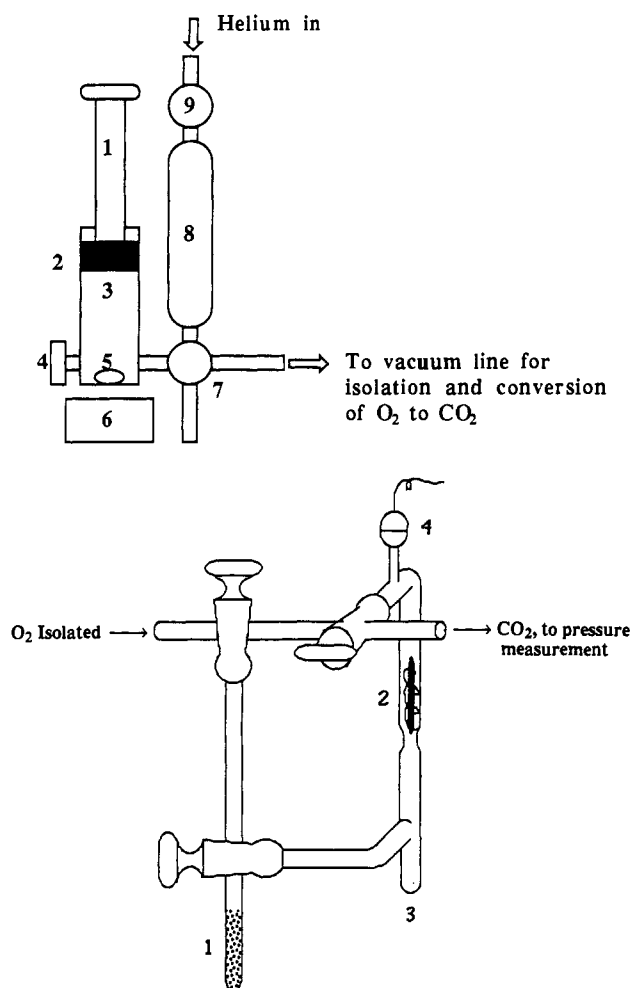


**Figure 1.** (A, top) The device used to introduce solution samples into the vacuum line for isolation and conversion of O<sub>2</sub> to CO<sub>2</sub>: (1) plunger stem; (2) rubber piston; (3) body of a syringe-like glass container; (4) rubber seal; (5) stirring bar; (6) stirring plate; (7) fourway vacuum valve; (8) glass tube of fixed volume; (9) two-way vacuum valve. (B, bottom) The loop furnace for conversion of O<sub>2</sub> to CO<sub>2</sub>: (1) molecular sieve trap; (2) a graphite wrapped in a platinum wire; (3) a liquid nitrogen trap for condensation of CO<sub>2</sub>; (4) a vacuum gauge head.

### Methods. (a) Determination of $\lambda_{\max}$ and Extinction Coefficients for the $\gamma$ Band of the Ferrous and Ferric Forms of Hemoglobin and Myoglobin.

In order to prepare ferrous forms of protein, ferric protein (ca. 20 mg in 0.5 mL) was first dialyzed against 4 L of 0.010 M Tris-HCl, pH 7.8, overnight. Any precipitate was removed by centrifugation. An approximately 1.2 molar excess of sodium dithionite was added to the protein solution, and the resulting mixture was immediately passed through a desalting column equilibrated with the Tris buffer. The eluted protein was collected and stored on ice. Ferric proteins were prepared by the same procedure except that the reduction by dithionite was omitted. Samples of ferric and ferrous hemoglobin in 0.010 M phosphate buffer, pH 6.5, were also prepared by the above procedure.

The iron content of ferrous and ferric protein samples was determined by atomic absorption spectroscopy. Iron solutions of different concentrations were prepared by dilution of a standard iron solution of known concentration in doubly distilled water; a standard curve was made by plotting  $A_{238.4}$  values vs the concentration of the iron solutions. The iron concentration of protein was calculated from its  $A_{238.4}$ , after correction for the absorbance of buffer.

The UV-visible spectra of the same ferrous and ferric samples were measured to obtain absorbance at the  $\gamma$  band<sup>4</sup> under the conditions of our experiments. Extinction coefficients were calculated on the basis of the iron concentration derived from atomic absorption spectroscopy.

(b) **Measurement of Isotope Effects.** The vacuum apparatus constructed for the isotopic measurements was composed of a syringe-like container for introducing a solution sample into the vacuum line (Figure 1A), a vacuum line for isolation of O<sub>2</sub> from the solution sample, and a

furnace for the conversion of the isolated O<sub>2</sub> to CO<sub>2</sub> (Figure 1B). Isolation and conversion of O<sub>2</sub> to CO<sub>2</sub> was carried out by a modification of the method of Guy et al.<sup>2</sup> Immediately before the start of an isotopic experiment, a protein stock solution was allowed to warm up to room temperature for 20 min with stirring. It was then injected through a rubber seal into the syringe-like container filled with a buffer solution. The following steps were operated under vacuum. After being mixed well, the protein solution (with a concentration usually in the range of 0.2–0.5 mM) in the syringe-like container was delivered to a pre-evacuated glass tube of fixed volume (ca. 30 mL) through the four-way valve (Figure 1A). Under a stream of purified helium, the solution in the glass tube was delivered to a round-bottom flask in the vacuum line that was immersed in a water bath at room temperature. This sample was then purged with helium for 3 min with stirring, followed by evacuation with a high-vacuum pump for 15 min. The above procedure was repeated two more times. The water and carbon dioxide that evolved were removed with three cold traps at liquid nitrogen temperature. The O<sub>2</sub> and N<sub>2</sub> mixture which evolved from the purging and evacuation cycles was trapped in molecular sieves (5 Å) at liquid nitrogen temperature. After being released from the molecular sieves, this mixture was transferred to the O<sub>2</sub>–CO<sub>2</sub> conversion furnace (Figure 1B). The furnace was shaped as a loop so that the gas mixture inside the loop could circulate upon heating; this configuration shortened the time required for the complete conversion. The conversion was carried out over hot graphite wrapped in a platinum wire and was usually complete within 20 min at ca. 900 °C. The newly formed CO<sub>2</sub> was transferred to an isolated glass container of fixed volume and the pressure which the CO<sub>2</sub> sample generated was measured with a pressure transducer. The CO<sub>2</sub> sample was then sealed in a glass tube and shipped to Krueger Enterprises (Cambridge, MA), where the value of the <sup>18</sup>O to <sup>16</sup>O ratio was determined by mass ratio spectrometry. Isolation and conversion of O<sub>2</sub> to CO<sub>2</sub> for blank samples were carried out in the same way.

(c) **Theory for Determination of Equilibrium Isotope Effects.** For the oxygen binding reaction



where P is an oxygen-carrier protein, the equilibrium isotope effect may be expressed as

$$^{18}(K)_{\text{obs}} = R_o/R_p \quad (2)$$

where  $R_o = [^{18}\text{O}_2]/[^{16}\text{O}_2]$  and  $R_p = [\text{P}_r \cdot ^{18}\text{O}_2]/[\text{P}_r \cdot ^{16}\text{O}_2]$ .

In an open system where dissolved oxygen is at isotopic equilibrium with air,  $R_o$  is constant whether an oxygen-carrier protein is present or not. Therefore, the value of  $R_o$  can be determined by mass ratio analysis of O<sub>2</sub> isolated from a blank sample. Although the value of  $R_p$  cannot be determined directly, it is related to an apparent isotopic ratio,  $R_{p(\text{app})}$ :

$$R_{p(\text{app})} = \frac{[^{18}\text{O}_2] + [\text{P}_r \cdot ^{18}\text{O}_2]}{[^{16}\text{O}_2] + [\text{P}_r \cdot ^{16}\text{O}_2]} \quad (3)$$

Multiplying both the numerator and the denominator of the right side of eq 3 with  $[\text{P}_r \cdot ^{16}\text{O}_2]/[^{16}\text{O}_2]$  and rearranging yields  $R_p$  in terms of  $R_{p(\text{app})}$  and  $R_o$ :

$$R_p = R_{p(\text{app})} + [R_{p(\text{app})} - R_o] \frac{[^{16}\text{O}_2]}{[\text{P}_r \cdot ^{16}\text{O}_2]} \quad (4)$$

Since the isotopic experiments in this work involved oxygen containing the natural abundance of <sup>18</sup>O<sub>2</sub> (0.2% per O; 0.4% per O<sub>2</sub>),  $[\text{P}_r \cdot ^{16}\text{O}_2]$  and  $[\text{P}_r \cdot ^{18}\text{O}_2]$  may be approximated by  $[\text{P}_r \cdot \text{O}_2]$  and  $[\text{O}_2]$ . Using the relationship  $[\text{P}_r \cdot \text{O}_2] = [\text{O}_{2T}] - [\text{O}_2]$ , where  $[\text{O}_{2T}]$  is the total O<sub>2</sub> concentration in the sample solution, one arrives at

$$R_p = R_{p(\text{app})} + [R_{p(\text{app})} - R_o] \frac{f}{1-f} \quad (5)$$

where  $f = [\text{O}_2]/[\text{O}_{2T}]$ . Bringing eq 5 into eq 2 leads to the expression for the isotope effect.

$$^{18}(K)_{\text{obs}} = \frac{1-f}{R_{p(\text{app})}/R_o - f} \quad (6)$$

(d) **Computation of Equilibrium Isotope Effects.** Theoretically, an equilibrium isotope effect (EIE) can be expressed as a product of three terms, contributed from the zero-point energies (ZPE), excited vibration

states (EXC), and the mass and moments of inertia (MMI):<sup>7</sup>

$$\text{EIE} = \text{ZPE} \times \text{EXC} \times \text{MMI} \quad (7)$$

For calculated oxygen isotope effects ( $^{18}(K)_{\text{calc}}$ ), these terms are related to vibrational frequencies of <sup>16</sup>O reactant ( $\nu_{16(r)}$ ), <sup>18</sup>O reactant ( $\nu_{18(r)}$ ), <sup>16</sup>O product ( $\nu_{16(p)}$ ), and <sup>18</sup>O product ( $\nu_{18(p)}$ ) through the relationships

$$\text{ZPE} = \exp\left(\frac{h}{2kT} \left[ \sum_i^{3n-6} [(\nu_{16(r)})_i - (\nu_{18(r)})_i] - \sum_i^{3n-6} [(\nu_{16(p)})_i - (\nu_{18(p)})_i] \right] \right) \quad (8)$$

$$\text{EXC} = \prod_i^{3n-6} \frac{1 - \exp\left[-\frac{h}{kT}(\nu_{16(r)})_i\right]}{1 - \exp\left[-\frac{h}{kT}(\nu_{18(r)})_i\right]} \prod_i^{3n-6} \frac{1 - \exp\left[-\frac{h}{kT}(\nu_{18(p)})_i\right]}{1 - \exp\left[-\frac{h}{kT}(\nu_{16(p)})_i\right]} \quad (9)$$

and

$$\text{MMI} = \prod_i^{3n-6} \frac{(\nu_{18(r)})_i}{(\nu_{16(r)})_i} \prod_i^{3n-6} \frac{(\nu_{16(p)})_i}{(\nu_{18(p)})_i} \quad (10)$$

where  $h$  is Planck's constant,  $k$  the Boltzmann constant, and  $T$  the absolute temperature.

For H<sub>2</sub>O<sub>2</sub> and H<sub>2</sub>O, the  $\nu_{16}$  and  $\nu_{18}$  values were calculated by using known force constants and the method for the calculation of Wilson et al.<sup>8</sup> A modified version of the computer program BEBOVIB-IV<sup>45</sup> was used for this purpose. For all other molecules, the  $\nu_{16}$  values were from literature, and the isotopic frequencies were computed by using the relationship

$$\nu_{18} = \nu_{16} \sqrt{\frac{G_{18}}{G_{16}}} \quad (11)$$

where  $G$  is the corresponding diagonal  $G$  element in the  $G$  matrix defined by Wilson et al.<sup>8</sup>

## Results and Discussion

**Demonstration of Quantitative Recovery of O<sub>2</sub> from Protein–O<sub>2</sub> Complexes.** As shown in eq 6, determination of  $^{18}(K)_{\text{obs}}$  requires accurate measurement of  $R$  and  $f$ . Through isotope ratio mass spectrometric techniques,  $R_o$  and  $R_{p(\text{app})}$  can be measured with high precision. Additionally, using a pressure transducer to measure CO<sub>2</sub> derived from O<sub>2</sub>, quantitation of O<sub>2</sub> in reaction samples is possible. Systematic errors in both  $f$  and  $R$  can, however, arise from incomplete isolation of oxygen from reaction mixtures. As described under Methods, removal of oxygen from reaction samples is accomplished by helium purging and high-vacuum evacuation. With regard to blank reactions, isolation of oxygen has been shown to be quantitative, as indicated by the fact that extended time dedicated to purging and evacuation did not increase the amount of O<sub>2</sub> isolated; further, the yield by helium purging and high-vacuum evacuation was identical with that obtained by helium sparging.<sup>2</sup>

The question remained whether oxygen isolated in the presence of oxygen carrier proteins would also be quantitative. Although the amount of oxygen isolated from the reaction mixtures can be accurately determined from the pressure of the CO<sub>2</sub> derived from O<sub>2</sub>, the initial concentration of O<sub>2</sub> in incubations was expected to be a function of the fraction of total protein containing bound O<sub>2</sub>. Given the high concentration of protein used in these experiments (mM range) in relation to their affinities for O<sub>2</sub> (μM range), less than full occupancy by O<sub>2</sub> would only arise if protein samples were contaminated by protein forms unable to bind O<sub>2</sub> effectively. This turned out to be a consideration only

(7) Melander, L.; Saunders, W. H. *Reaction Rates of Isotopic Molecules*; Wiley: New York, 1980.

(8) Wilson, E. B., Jr.; Decius, J. C.; Cross, P. C. *Molecular Vibrations, The Theory of Infrared and Raman Vibrational Spectra*; Dover Publications: New York, 1955.

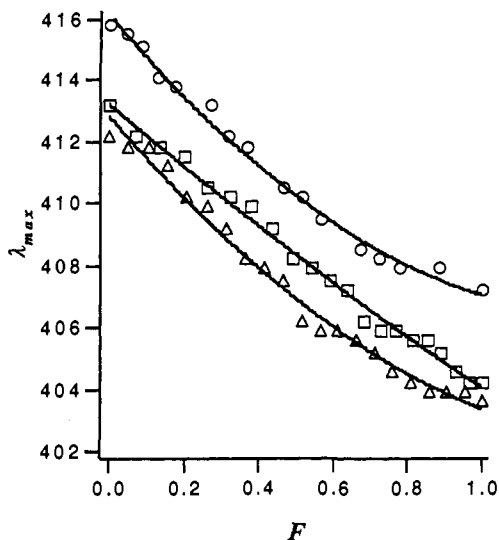


**Figure 2.** Plots of the apparent maximum wavelength ( $\lambda_{\max}$ ) of the  $\gamma$  band vs the fraction of ferric species in a mixture of ferrous and ferric myoglobin at pH 7.8 (O), hemoglobin at pH 6.5 ( $\Delta$ ), and hemoglobin at pH 7.8 ( $\square$ ).

in the case of myoglobin and hemoglobin, which generally contained some ferric form under our experiment conditions. In the course of our experiments, the ferrous forms of myoglobin and myoglobin were generated by reduction of the ferric species with dithionite. To avoid possible contamination of final solutions by dithionite, a slightly less than stoichiometric amount of reductant was routinely used, which led to a limited amount of contaminating ferric species. Additionally, some autooxidation was anticipated in the course of protein isolation and manipulation.<sup>9</sup>

The concentration of the ferrous species in myoglobin and hemoglobin samples containing certain amounts of ferric forms could not be determined in a simple manner from the absorbance of  $\alpha$  and  $\beta$  bands, due to considerable tailing of the  $\gamma$  band of the ferric form in this region. We therefore employed an empirical method for the estimation of the amount of ferric species in myoglobin and hemoglobin solutions. A series of samples with varying percentages of ferric heme proteins were prepared by mixing known amounts of ferrous and ferric protein. Spectra of these mixtures were obtained, allowing estimation of  $\lambda_{\max}$  for the  $\gamma$  band as a function of the ratio of ferric to total heme protein ( $F$ ). The resulting data, shown in Figure 2, could be fit to the following empirical equation,  $\lambda_{\max} = a + bF + cF^2$ , where  $a$ ,  $b$ , and  $c$  are constants. From this relationship, the value of  $F$  was determined from the experimental  $\lambda_{\max}$  observed with myoglobin and hemoglobin preparations employed in isotope effect measurements. In the course of these studies an apparent extinction coefficient of the  $\gamma$  band was also determined at each  $F$  value, by division of the absorbance at an observed  $\lambda_{\max}$  by the concentration of protein. The resulting relationship between  $\epsilon$  and  $F$  is shown in Figure 3, which could be fit to  $\epsilon = a + bF + cF^2 + dF^3$ , where  $a$ ,  $b$ ,  $c$ , and  $d$  are a new set of constants. Experimental samples were first analyzed for an observed  $\lambda_{\max}$  and attendant  $F$  value (Figure 2). Protein concentrations were estimated from  $F$  and the data in Figure 3. Finally, the concentration of ferrous protein in each experimental sample could be obtained from  $F$  and total protein concentration.

With this information in hand, it became possible to determine the efficiency of oxygen isolation from samples containing oxyhemoglobin and oxymyoglobin. The correlation of the pressure of  $\text{CO}_2$  derived from isolated  $\text{O}_2$  with the concentration of the ferrous myoglobin or hemoglobin is shown in Figure 4. Since pressure units are arbitrary, we set the value at 20.0 using buffer samples containing 0.258 mM  $\text{O}_2$ . Significantly, the experimental

(9) Brooks, J. *Proc. R. Soc. B* 1931, 109, 35.

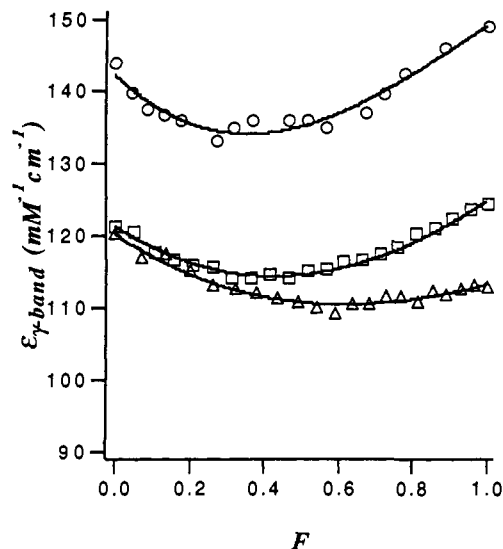


**Figure 3.** Plots of apparent extinction coefficients  $\epsilon$  of the  $\gamma$  band vs the fraction of ferric species in a mixture of ferrous and ferric myoglobin at pH 7.8 (O), hemoglobin at pH 6.5 ( $\Delta$ ), and hemoglobin at pH 7.8 ( $\square$ ).

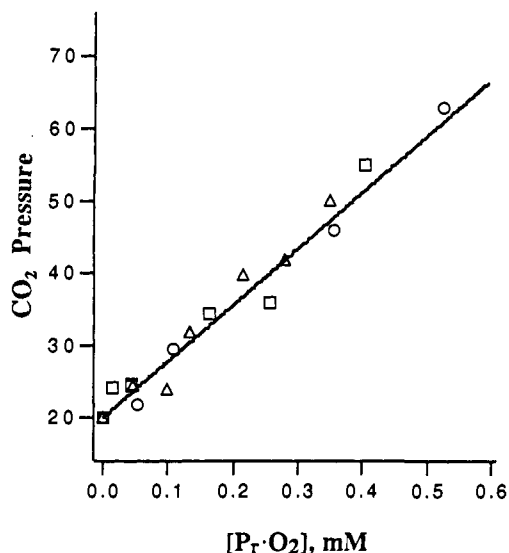


**Figure 4.**  $\text{CO}_2$  pressure data at corresponding concentrations of oxygenated protein,  $\text{P}_r\cdot\text{O}_2$ : oxymyoglobin at pH 7.8 (O), hemoglobin at pH 6.5 ( $\Delta$ ), and hemoglobin at pH 7.8 ( $\square$ ). The line is calculated by using 20.0  $\text{CO}_2$  pressure units equal to 0.258 mM  $\text{O}_2$ . See text for more details.

data in Figure 4 are evenly distributed around a theoretical line which has been drawn by using the relation of 20.0 pressure units = 0.258 mM, indicative of full recovery of  $\text{O}_2$  from protein- $\text{O}_2$  complexes. Data were recollected with hemoglobin at pH 6.5, conditions which reduce the affinity of  $\text{O}_2$  ca. 10-fold relative to pH 7.8.<sup>10,11</sup> As shown, data at pH 6.5 and 7.8 are virtually indistinguishable. Similarly, data collected with 5 mM diphosphoglycerate, a regulator of hemoglobin that reduces the affinity of  $\text{O}_2$ ,<sup>12</sup> were not detectably higher than those obtained in the absence of diphosphoglycerate, a further indication that isolation of  $\text{O}_2$  from protein- $\text{O}_2$  complexes is quantitative. In light of these results, the isolation efficiency was not determined in experiments with hemocyanin and hemerythrin. It is known that the affinity of  $\text{O}_2$  for hemocyanin ( $K_d = 3.6 \times 10^{-6}$  M, pH 7)<sup>13</sup>

(10) Antonini, E.; Wyman, J.; Brunori, M.; Fronticelli, C.; Bucci, E.; Fanelli, A. R. *J. Biol. Chem.* 1969, 240, 1096-1103.

(11) Imai, K.; Yonetani, T. *J. Biol. Chem.* 1975, 250, 2227-2231.

(12) Benesch, R.; Benesch, R. E. *Nature* 1969, 221, 619-622.

(13) Sullivan, B.; Bonaventura, J.; Bonaventura, C. *Proc. Natl. Acad. Sci. U.S.A.* 1974, 71, 2558-2562.

Table I. Summary of Equilibrium Isotope Effects

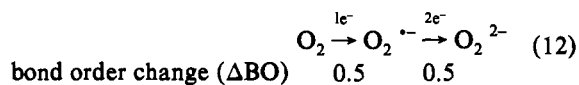
protein	<i>f</i>	<i>R<sub>p(app)</sub>/R<sub>o</sub></i>	<sup>18</sup> ( <i>K</i> ) <sub>obs</sub> <sup>a</sup>
myoglobin	0.4417	0.9970	1.0055
	0.4348	0.9972	1.0050
	0.3175	0.9961	1.0058
			1.0054 ± 0.0006
hemoglobin	0.4000	0.9976	1.0040
	0.5000	0.9982	1.0036
	0.4762	0.9979	1.0041
			1.0039 ± 0.0002
hemerythrin	0.4739	0.9943	1.0110
	0.4651	0.9938	1.0117
	0.4902	0.9941	1.0117
	0.4739	0.9941	1.0113
	0.4762	0.9947	1.0102
	0.4651	0.9938	1.0117
		1.0113 ± 0.0005	
hemocyanin	0.5195	0.9923	1.0163
	0.5025	0.9908	1.0188
	0.4000	0.9907	1.0157
	0.4082	0.9892	1.0186
	0.4494	0.9899	1.0187
	0.4546	0.9891	1.0204
	0.5226	0.9904	1.0205
			1.0184 ± 0.0023

<sup>a</sup> Final values are the average of replicate measurements. Experimental reproducibility varies from 11% with myoglobin (0.06/0.54 × 100) to 4.4% with hemerythrin.

and hemerythrin (*K<sub>d</sub>* = 6.7 × 10<sup>-6</sup> M, pH 8.2)<sup>14</sup> is not significantly different from the affinity of O<sub>2</sub> for myoglobin (*K<sub>d</sub>* = 0.9 × 10<sup>-6</sup> M, pH 7.7)<sup>15</sup> and hemoglobin, pH 8 (*K<sub>d</sub>* = 3.8 × 10<sup>-6</sup> M).<sup>11</sup> It was therefore assumed that the O<sub>2</sub> isolation procedures used with myoglobin and hemoglobin would lead to complete O<sub>2</sub> recovery in the case of hemocyanin and hemerythrin.

**The Magnitude of Equilibrium Isotope Effects.** Experimentally measured values of *R<sub>p(app)</sub>/R<sub>o</sub>*, *f*, and <sup>18</sup>(*K*)<sub>obs</sub> are summarized in Table I. It can be seen that final values for <sup>18</sup>O isotope effects are quite reproducible, with experimental errors that are significantly less than the size of the individual isotope effects. The size of <sup>18</sup>(*K*)<sub>obs</sub> is found to decrease from 1.8% to 0.4% in proceeding from the more ancestral O<sub>2</sub> carrier proteins, hemocyanin and hemerythrin, to myoglobin and hemoglobin. This almost 5-fold change in magnitude is very significant and can, in principle, provide insight into the mode of binding of O<sub>2</sub> to each of the carrier proteins.

Data in the literature are consistent with a formal reduction of O<sub>2</sub> to either superoxide in myoglobin<sup>16</sup> and hemoglobin<sup>17</sup> or peroxide in hemocyanin<sup>18</sup> and hemerythrin.<sup>19</sup> As summarized in eq 12, reductions of this nature produce net bond order changes of 0.5 and 1.0, respectively, predicting significant larger isotope effects than are actually observed.



This indicates that compensating factors, involving metal-oxygen interactions and/or protonation at oxygen, are contributing to the experimentally observed values of Table I.

In order to provide a more quantitative context for the interpretation of oxygen isotope effects, we have carried out isotope

(14) DeWall, D. J. A.; Wilkins, R. G. *J. Biol. Chem.* **1976**, *251*, 2339-2343.

(15) Projahn, H.-D.; Dreher, C.; van Eldik, R. *J. Am. Chem. Soc.* **1990**, *112*, 17-22.

(16) Maxwell, J. C.; Volpe, J. A.; Barlow, C. H.; Caughey, W. S. *Biochem. Biophys. Res. Commun.* **1974**, *58*, 166-171.

(17) Barlow, C. M.; Maxwell, J. C.; Wallace, W. J.; Caughey, W. S. *Biochem. Biophys. Res. Commun.* **1973**, *55*, 91-95.

(18) Loehr, J. S.; Freedman, T. B.; Loehr, T. M. *Biochem. Biophys. Res. Commun.* **1974**, *56*, 510-515.

(19) Dunn, J. B. R.; Shriver, D. F.; Klotz, I. M. *Proc. Natl. Acad. Sci. U.S.A.* **1973**, *70*, 2582-2584.

Table II. Vibrational Frequencies (cm<sup>-1</sup>) of Symmetric Species

molecule	mode	$\nu_{16}^a$	$\nu_{18}^b$
O <sub>2</sub>		1556.3	1512.5
O <sub>2</sub> <sup>•-</sup>		1064.8	1034.8
O <sub>2</sub> <sup>2-</sup>		800	777.0
H <sub>2</sub> O <sub>2</sub> <sup>c</sup>	H-O	3606.4	3604.5
		3604.4	3593.1
	H-O-O	1396.7	1394.2
H <sub>2</sub> O <sup>c</sup>	O-O	1264.9	1262.4
		863.3	839.3
	torsion	320.2	319.8
	H-O	3824	3824
	H-O-H	3939	3922
		1654	1644

<sup>a</sup>  $\nu_{16}$  values for O<sub>2</sub> and O<sub>2</sub><sup>•-</sup> were taken from Chase et al.<sup>40</sup> The value for O<sub>2</sub><sup>2-</sup> was from Evans.<sup>41</sup> <sup>b</sup>  $\nu_{18}$  values for the three diatomic species were calculated by using the following relationship:  $\nu_{18} = \nu_{16}(G_{18}/G_{16})^{1/2}$ , where *G* is the corresponding diagonal *G* element in the *G* matrix (see under Methods). <sup>c</sup> All of these values were calculated by using known force constants for H<sub>2</sub>O<sub>2</sub><sup>42</sup> and H<sub>2</sub>O.<sup>43</sup>

Table III. Vibrational Frequencies (cm<sup>-1</sup>) of Asymmetric Species

molecule	mode	$\nu_{16}^a$	$\nu_{18t}^b$	$\nu_{18c}^b$
HO <sub>2</sub> <sup>•</sup>	H-O	3433.0	3433.0	3421.4
	O-O	1103.9	1071.8	1074.6
	H-O-O	1390.8	1388.4	1383.6
HO <sub>2</sub> <sup>-</sup>	H-O	3539	3539	3527
	O-O	755	734	734
	H-O-O	1205	1204	1199

<sup>a</sup>  $\nu_{16}$  values for HO<sub>2</sub><sup>•</sup> were from Smith and Andrew<sup>20</sup> and the values for HO<sub>2</sub><sup>-</sup> were from Oakes et al.<sup>44</sup> <sup>b</sup>  $\nu_{18t}$  and  $\nu_{18c}$  are vibrational frequencies for species with <sup>18</sup>O at the terminal and central positions, respectively. They were calculated by using the following relationship:  $\nu_{18} = \nu_{16}(G_{18}/G_{16})^{1/2}$ , assuming the off-diagonal elements of the *G* matrix are negligible (see text).

effect calculations for the species O<sub>2</sub><sup>•-</sup>, HO<sub>2</sub><sup>•</sup>, O<sub>2</sub><sup>2-</sup>, HO<sub>2</sub><sup>-</sup>, H<sub>2</sub>O<sub>2</sub>, and H<sub>2</sub>O. As indicated under Methods, it is necessary to know the vibrational frequencies for both <sup>16</sup>O and <sup>18</sup>O species in order to calculate isotope effects. The values of  $\nu_{16}$  and  $\nu_{18}$  employed in calculations of oxygen isotope effects are summarized in Tables II and III. The  $\nu_{16}$  values are all known in the literature. While literature data for  $\nu_{18}$  are limited, these can be calculated from  $\nu_{16}$  in a straightforward fashion for diatomic species (Table II). For H<sub>2</sub>O<sub>2</sub> and H<sub>2</sub>O, a set of force constants is available, from which both  $\nu_{16}$  and  $\nu_{18}$  values could be obtained (Table II). For HO<sub>2</sub><sup>-</sup>, no force constants have been reported: in this case, the  $\nu_{18}$  values were calculated by using the literature values of  $\nu_{16}$ , assuming that the off-diagonal elements of the *G* matrix<sup>8</sup> contribute little to the vibrational frequencies. To test the validity of this assumption, the simplified procedure was also applied to the calculations for HO<sub>2</sub><sup>•</sup>, for which both  $\nu_{16}$  and  $\nu_{18}$  values are known.<sup>20</sup> We find that values for <sup>18</sup>(*K*)<sub>calc</sub> obtained from estimated and known  $\nu_{18}$  values for HO<sub>2</sub><sup>•</sup> agree reasonably well: 1.011 47 (Table IV) and 1.010 13, respectively.

As described under Methods, isotope effect calculations provide estimates of the three terms contributing to <sup>18</sup>(*K*)<sub>calc</sub>. These terms, which arise from changes in ground-state vibrational modes between reactant and product (ZPE), changes in excited-state vibrational modes (EXC), and changes in mass and moments of inertia (MMI), are summarized in Table IV along with the final values for the isotope effects, <sup>18</sup>(*K*)<sub>calc</sub>. Also summarized in Table IV are the changes in bond order occurring upon the uptake of electrons and protons at oxygen to generate each of the species studied. For the two reactions where dioxygen is converted to the asymmetric triatomic species, HO<sub>2</sub><sup>•</sup> and HO<sub>2</sub><sup>-</sup>, the <sup>18</sup>O label can be at either the central or terminal position. The populations of the two isotopic products are expected to be close to each other. Therefore, the apparent oxygen-18 isotope effect was calculated assuming equal populations of the two isotopic species.

(20) Smith, D. W.; Andrew, L. *J. Chem. Phys.* **1974**, *60*, 81-85.

Table IV. Calculated Equilibrium Isotope Effects

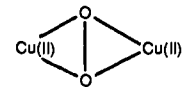
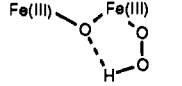
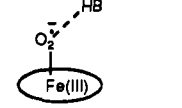
reaction	$\Delta BO/O$ atom	$^{18}(K)_{\text{calc}}$	ZPE	EXC	MMI
$O_2 \xrightleftharpoons{2e^-} O_2^{2-}$	1	1.049 62	1.051 47	0.997 61	1.000 63
$O_2 \xrightleftharpoons{1e^-} O_2^{\cdot -}$	0.5	1.033 09	1.033 86	0.999 21	1.000 04
$O_2 \xrightleftharpoons{2e^-, H^+} HO_2^-$	0.5				
$H^{16}O-^{18}O$		1.051 64	1.054 01	0.997 25	1.000 50
$H^{18}O-^{16}O$		1.016 96	1.011 65	0.997 18	1.008 09
Net:		1.034 01 <sup>a</sup>			
$O_2 \xrightleftharpoons{1e^-, H^+} HO_2^{\cdot}$	0				
$H^{16}O-^{18}O$		1.023 49	1.022 64	0.999 32	1.001 46
$H^{18}O-^{16}O$		0.999 72	0.999 52	0.999 29	1.000 91
Net:		1.011 47 <sup>a</sup>			
$O_2 \xrightleftharpoons{2e^-, 2H^+} H_2O_2$	0	1.008 90	1.002 90	0.997 63	1.008 37
$O_2 \xrightleftharpoons{4e^-, 4H^+} 2H_2O$	0	1.022 75	1.041 37	1.000 11	0.982 01

<sup>a</sup> As pointed out by a referee, the formal relationship between the final isotope effect and the effect obtained from each species of bound oxygen (e.g.,  $^{16}O-^{18}O$  and  $^{18}O-^{16}O$ ) is  $^{18}(K)_{\text{calc}} = 2 / (^{18}K_1^{-1} + ^{18}K_2^{-1})$ . Simple averaging of  $^{18}K_1$  and  $^{18}K_2$  leads to similar results when values for the isotope effects are in the range of these studies, e.g., 1.03430 for  $HO_2^-$  production and 1.01161 for  $HO_2^{\cdot}$  production.

The data in Table IV fall into two categories involving either a 0.5–1.0 change in bond order or a conservation in bond order. Examining the three examples where bond order is reduced, it is possible to obtain an average isotope effect of 1.029 25 for a reduction of bond order of 0.5 at oxygen. Turning to the two examples where the  $\pi$  bond of  $O=O$  is converted to  $O-H$  with conservation of bond order at oxygen, normal isotope effects are observed, providing an average value of 1.009 62. It can be seen that conversion of both the  $\pi$  and  $\sigma$  bonds in  $O=O$  to  $O-H$  ( $O_2 \rightleftharpoons 2H_2O$ ) leads to a value for  $^{18}(K)_{\text{calc}}$  that is approximately 2-fold greater than 1.009 62. That the isotope effects are normal is mainly a result of a significant reduction in the reduced mass. In the absence of force field analyses for the relevant copper and iron oxygen complexes, it is premature to attempt modeling experimental values representing the oxygen carrier proteins of Table I. However, substitution of a metal for a proton may produce a very small change since it brings about opposing effects of an increase in mass and decrease in force constant. In support of this view, calculations of isotope effects resulting solely from an  $O-H$  vs  $O-Cu^{II}$  or  $Fe^{III}$  bond stretching mode indicate virtually identical results (unpublished results).

**Relationship of Isotope Effects to Proposed Structures for the Oxygenated Forms of Hemocyanin, Hemerythrin, and Hemoglobin, and Myoglobin.** An extensive literature exists regarding the nature of oxygen binding to each of the reversible oxygen carriers found in nature. In the case of myoglobin and hemoglobin, the combination of X-ray crystallography,<sup>21</sup> neutron diffraction,<sup>22</sup> and infrared<sup>15,16,23</sup> techniques implicates a metal complexed oxygen species which is hydrogen bonded to a distal histidine (Table V). Both EPR and optical spectra on native and cobalt substituted heme proteins support the presence of the metal oxygen as a ferric-superoxide intermediate.<sup>24,25</sup> It is therefore of considerable interest that the measured equilibrium isotope effects,  $1.0039 \pm 0.002$  for hemoglobin and  $1.0054 \pm 0.006$  for myoglobin, are smaller than the value of 1.011 47, the isotope effect calculated for protonated superoxide,  $HO_2^{\cdot}$ . Although isotope effects are

Table V. Structures for  $O_2$  Complexes

protein	proposed structures	bonding <sup>a</sup>
Hc		$H_2O_2 < Hc < HO_2^{\cdot}$ 1.0089 < 1.0184 < 1.0343
Hr		$H_2O_2 = Hr$ 1.0089 $\approx$ 1.0113
Hb <sup>b</sup>		$Hb < HO_2^{\cdot}$ 1.0039 < 1.0103

<sup>a</sup> Comparison of values for  $^{18}(K_{\text{eq}})_{\text{calc}}$ , Table IV, to  $^{18}(K_{\text{eq}})_{\text{obs}}$ , Table I. <sup>b</sup> The heme coordinated to iron is represented by a circle; HB represents the protonated distal histidine.

not available for the formation of model metal superoxide complexes, it is possible that these will be similar to the value calculated for  $HO_2^{\cdot}$ . We therefore attribute the reduction in the experimental isotope effects for hemoglobin and myoglobin, relative to protonated superoxide, to an increased bonding to oxygen. The simplest explanation for this phenomenon is the presence of a hydrogen bond from the distal histidine. Shaanan<sup>21</sup> noticed that in the  $\alpha$  subunit of hemoglobin, the distance between the nitrogen atom of the distal histidine side chain and the terminal oxygen atom of dioxygen bound to iron is 2.7 Å, shorter than that in myoglobin (3.0 Å). Although the  $\beta$  subunit of hemoglobin shows longer distances between the nitrogen of the distal histidine (ca. 3.3 Å) and both oxygen atoms of bound dioxygen, the net hydrogen bonding to hemoglobin may be stronger than that in myoglobin. In support of this view, the equilibrium isotope effect in hemoglobin is smaller than that in myoglobin by a small but significant fraction (ca. 27% of the 0.54% isotope effect).

The data for oxygen binding to hemerythrin can also be interpreted in the context of studies by X-ray crystallography,<sup>26,27</sup> X-ray absorption spectroscopy,<sup>28</sup> single-crystal polarized absorbance spectroscopy,<sup>29</sup> and resonance Raman,<sup>30–32</sup> which implicate the presence of iron hydrogen peroxide hydrogen bonded to the bridge oxygen of the  $\mu$ -oxo-bridged diferric species (Table V). We note that the experimentally determined equilibrium isotope effect for hemerythrin is close to the computed value for  $H_2O_2$ . The experimental value is slightly larger than the calculated value, consistent with the known structure in which the  $O-H$  bond of  $Fe^{III}-OOH$  is weakened by hydrogen bonding to the bridging oxygen.

Turning to the structure of oxyhemocyanin, this has been the most controversial, in large part resulting from the absence of an X-ray structure for oxyhemocyanin. Proposed structures for the  $\mu$ -peroxy-bridged dicopper complex have ranged from a *cis*  $\mu$ -1,2 coordination with the possibility of an additional endogenous bridging ligand to the copper atoms<sup>33</sup> to a coordination described as  $\mu$ - $\eta^2$ : $\eta^2$  (ref 34, as shown in Table V). The *cis*  $\mu$ -1,2 coordination might be expected to yield an equilibrium isotope effect similar

(26) Stenkamp, R. E.; Sieker, L. C.; Jensen, L. H. *J. Am. Chem. Soc.* **1984**, *106*, 618–622.

(27) Stenkamp, R. E.; Sieker, L. C.; Jensen, L. H.; McCallum, J. D.; Sanders-Loehr, J. *Proc. Natl. Acad. Sci. U.S.A.* **1985**, *82*, 713–716.

(28) Elam, W. T.; Stern, E. A.; McCallum, J. D.; Sanders-Loehr, J. *J. Am. Chem. Soc.* **1982**, *104*, 6369–6373.

(29) Reem, R. C.; McCormick, J. M.; Richardson, D. E.; Devlin, F. J.; Stephens, P. J.; Musselman, R. L.; Solomon, E. I. *J. Am. Chem. Soc.* **1989**, *111*, 4688–4704.

(30) Shiemke, A. K.; Loehr, T. M.; Sanders-Loehr, J. *J. Am. Chem. Soc.* **1984**, *106*, 4951–4956.

(31) Shiemke, A. K.; Loehr, T. M.; Sanders-Loehr, J. *J. Am. Chem. Soc.* **1986**, *108*, 2437–2443.

(32) Freier, S. M.; Duff, L. L.; Shriver, D. F.; Klotz, I. M. *Arch. Biochem. Biophys.* **1980**, *205*, 449–463.

(33) Himmelwright, R. S.; Eickman, N. C.; Solomon, E. I. *J. Am. Chem. Soc.* **1979**, *101*, 1576–1586.

(21) Shaanan, B. *Nature* **1982**, *296*, 683–684.

(22) Phillips, S. E. V.; Schoenborn, B. P. *Nature* **1981**, *292*, 81–82.

(23) Collman, J. P.; Brauman, J. I.; Halbert, T. R.; Suslick, K. S. *Proc. Natl. Acad. Sci. U.S.A.* **1976**, *73*, 3333–3337.

(24) Wittenberg, J. B.; Wittenberg, B. A.; Peisach, J.; Blumberg, N. E. *Proc. Natl. Acad. Sci. U.S.A.* **1970**, *67*, 1846–1853.

(25) Hoffman, B. M.; Petering, D. H. *Proc. Natl. Acad. Sci. U.S.A.* **1970**, *67*, 637–643.

to that for  $\text{H}_2\text{O}_2$ , whereas the actual value for oxyhemocyanin is considerably larger. Given the recent evidence for a side-on,  $\mu\text{-}\eta^2\text{:}\eta^2$  complex in oxyhemocyanin,<sup>34</sup> analogous to the structure originally reported by Kitajima et al.,<sup>35</sup> the bonding in hemocyanin is unlike any simple species we have attempted to model. All one can say at the moment is that the bonding at oxygen in hemocyanin lies somewhere between that expected for a fully protonated neutral peroxide and a monoprotonated anionic peroxide intermediate.

**Further Applications of Oxygen Isotope Effect Data.** The availability of oxygen isotope effects for the reversible binding of oxygen to each of the biological oxygen carriers provides the reference background necessary for studies of oxygen activation by a range of enzyme systems. In the reactions catalyzed, for example, by metallo-monoxygenases, reversible binding of oxygen to an enzyme active site metal center is believed to be followed by reductive activation to yield an intermediate capable of substrate functionalization. In the case of two well-studied proteins, cytochrome P-450 and dopamine  $\beta$ -monoxygenase, data exist for the initial formation of either a heme-iron hydroperoxide<sup>36</sup> or a copper hydroperoxide<sup>37</sup> species, respectively. With the data in hand for the anticipated magnitude of  $^{18}\text{O}$  discrimination upon formation of intermediates of this type, the magnitude of kinetic isotope effects under conditions of enzyme turnover can provide insight into rate-limiting steps and catalytic intermediates. Preliminary data with dopamine  $\beta$ -monoxygenase indicate kinetic oxygen isotope effects that are dependent on substrate structure and which are substantially larger than the equilibrium binding limits established in Table I. From data of this nature, it has been postulated that a metal peroxide intermediate in dopamine  $\beta$ -monoxygenase catalysis must undergo further

reductive activation, prior to catalysis of hydrogen atom abstraction from the  $\beta$ -carbon of the substrate.<sup>38</sup>

The methodology and data presented in this study may also prove quite valuable in the area of physiology. For example, Epstein and Zeiri<sup>39</sup> have examined oxygen isotope effects associated with respiration in human subjects with various degrees of anemia and under conditions of exercise and smoking. Although the oxygen isotopic discrimination in  $\text{CO}_2$  formed from  $\text{O}_2$  *in vivo* is expected to be influenced by a variety of steps, such as oxygen diffusion through membranes, oxygen binding to hemoglobin, and subsequent chemical steps, knowledge of oxygen isotope effects on each of these steps may lead to insights regarding the molecular origins of respiratory and blood diseases. In this context, Epstein and Zeiri have already demonstrated dramatic changes in oxygen isotope fractionations with patients suffering from anemia. It has been suggested that reduced hemoglobin concentrations may lead to an at least partially rate limiting binding of oxygen to its carrier protein *in vivo*.<sup>39</sup>

**Acknowledgment.** Joseph Rucker is acknowledged for assistance in using BEBOVIB-IV for calculations of equilibrium isotope effects and for valuable discussions. This work was supported by grants from the National Institutes of Health to J.P.K. (GM 39296) and the American Heart Association to G.T. (91-34).

(38) Klinman, J. P.; Berry, J. A.; Tian, G. In *Bioinorganic Chemistry of Copper*; Karlin, K. D., Tyeklar, Z., Eds.; Chapman and Hall: London, 1993.

(39) Epstein, S.; Zeiri, L. *Proc. Natl. Acad. Sci. U.S.A.* **1988**, *85*, 1727-1731.

(40) Chase, M. W.; Curnett, J. L.; Downey, J. R.; McDonald, R. A.; Syverud, A. N.; Valenzuela, E. A. *J. Phys. Chem. Ref. Data* **1982**, *11*, 695-740.

(41) Evans, J. C. *Chem. Commun.* **1969**, 682-683.

(42) Giguere, P. A.; Srinivasan, T. K. K. *J. Raman Spectrosc.* **1974**, *2*, 125-132.

(43) Nakamoto, K. *Infrared and Raman Spectra of Inorganic and Coordination Compounds*; John Wiley: New York, 1978.

(44) Oakes, J. M.; Harding, L. B.; Ellison, G. B. *J. Chem. Phys.* **1985**, *83*, 5400-5406.

(45) Sims, L. B.; Burton, G.; Lewis, D. E. BEBOVIB-IV. Quantum Chemistry Program Exchange, Department of Chemistry, Indiana University, Bloomington, Indiana 47401, Program No. 337.

(34) Kitajima, N.; Fujisawa, K.; Fujimoto, C.; Moro-oka, Y.; Nashimoto, S.; Kitagawa, T.; Toriumi, K.; Tatsumi, K.; Nakamura, A. *J. Am. Chem. Soc.* **1992**, *114*, 1277-1291.

(35) Magnus, K. A.; Ton-That, H. L. In *Bioinorganic Chemistry of Copper*; Karlin, K. D., Tyeklar, Z., Eds.; Chapman and Hall: London, 1993.

(36) Coon, M. J.; White, B. E. In *Metal Ion Activation of Dioxygen*; Spiro, T. G., Ed.; Wiley: New York, 1980.

(37) Ahn, N.; Klinman, J. P. *Biochemistry* **1983**, *22*, 3096-3106.